



HAL
open science

Adhesive contact: a few comments on cohesive zone models and self-consistency

Etienne Barthel

► **To cite this version:**

Etienne Barthel. Adhesive contact: a few comments on cohesive zone models and self-consistency. The Journal of Adhesion, 2012, 88, pp.55-69. 10.1080/00218464.2011.611057 . hal-00594627

HAL Id: hal-00594627

<https://hal.science/hal-00594627>

Submitted on 20 May 2011

HAL is a multi-disciplinary open access archive for the deposit and dissemination of scientific research documents, whether they are published or not. The documents may come from teaching and research institutions in France or abroad, or from public or private research centers.

L'archive ouverte pluridisciplinaire **HAL**, est destinée au dépôt et à la diffusion de documents scientifiques de niveau recherche, publiés ou non, émanant des établissements d'enseignement et de recherche français ou étrangers, des laboratoires publics ou privés.

Adhesive contact: a few comments on cohesive zone models and self-consistency

E. Barthel¹

*Surface du Verre et Interfaces, CNRS/Saint-Gobain, UMR 125, 93330, Aubervilliers Cedex
France.*

Abstract

We comment on the use of cohesive zone models in the context of the adhesive contact of spheres. We also propose an alternative derivation of the double Hertz cohesive zone model proposed by Greenwood and Johnson (J. Phys. D - Appl. Phys. 3279 (1998)). Based on this example, and the derivation method we use, we discuss some features of adhesive contact models, with emphasis on the role of the additional, physically motivated, lengthscale introduced by the cohesive zone.

Keywords: adhesion, contact, JKR, DMT, cohesive zone models, double Hertz model.

Introduction

Cohesive zone models have been introduced in adhesive contact problems 20 years ago [1, 2]. They are useful to inject an additional lengthscale in adhesion problems. In some cases indeed the details of the adhesive interaction are significant, beyond the mere adhesion energy w .

For instance for the DMT-JKR transition [1], the decay length of the interaction controls the fine details of the macroscopic contact variables, although the impact of this additional lengthscale is limited: for instance, moderate variations of the adhesion force are found throughout the DMT-JKR transition.

¹etienne.barthel@saint-gobain.com

Things start to look different if the system size becomes of the order of the cohesive zone size. As an example cohesive zones are instrumental in the modelling of flaw insensitive adhesion [3, 4]. For macroscopic samples, the local contact edge lengthscale impacts the stress distribution locally, and will strongly affect the overall behavior when non-elastic material response must be taken into account. For plastic response the peak stress governs the deviation from elastic behaviour. For viscoelastic materials, the lengthscale combined with the contact edge velocity controls deformation rates and eventually dissipation [5, 6, 7, 8].

For these reasons it is useful to study cohesive zone models in the context of adhesive contact problems. A large number such models have been proposed [1, 9, 10]. Comparison of various cohesive zone models has demonstrated that they are equivalent to a very large extent [9]. It is therefore possible to use the simpler one, for instance regarding computational difficulties. A very simple – and numerically amenable – cohesive zone model has been proposed by Greenwood and Johnson in 1998 [10]. This so called double Hertz model has subsequently been used for more complex systems, especially viscoelastic [11]. The original derivation of the double Hertz model was carried out by scaling from the Hertz solution. In this paper we reconsider the double Hertz model in a slightly different context. We show how the double Hertz model can be derived using the auxiliary function method [12, 11]. Then we take advantage of its numerical simplicity to illustrate some generic features of adhesive contact models.

1. Standard models

We start from the contact of an elastic, frictionless and axisymmetric punch with a rigid plane. The convex punch shape is otherwise not specified. Negative stresses are taken as tensile.

The punch is loaded with force F which results in the development of a contact zone of radius a (Figure 1). The penetration δ is the rigid body displacement of the undeformed parts of the punch far away from the contact zone.

In the absence of adhesion (Hertzian contact), the penetration δ and force F can be calculated as a function of the contact radius a :

$$\delta = \delta_H(a) \quad (1)$$

$$F = F_H(a) \quad (2)$$

1.1. Attractive interactions – DMT model

Simply adding adhesive interaction stresses $\sigma(r)$ around the contact zone results in the following contact equations (Fig. 1)

$$\delta_{DMT} = \delta_H(a) \quad (3)$$

$$F_{DMT} = F_H(a) + F_{ext}(a) \quad (4)$$

where the outer force term

$$F_{ext}(a) = 2\pi \int_a^{+\infty} dr r \sigma(r) \quad (5)$$

is the force applied on the sphere by the interaction stresses.

The gap $h(r)$ is the normal distance between the flat surface and the surface of the deformed punch. If the cohesive stresses derive from an interaction potential $V(z)$ then

$$\sigma(r) = -\frac{dV}{dz}(h(r)) \quad (6)$$

The adhesive force $F_{ext}(a)$ can be calculated numerically [13]. The result is in fact strongly dependent upon geometry [14].

In the specific case of a sphere of radius R , however, the result is remarkably simple. If the interaction stresses are weak enough, we can expect limited deviation (Fig.2) of the gap from

$$h(r) \simeq \frac{r^2}{2R} \quad (7)$$

from which, to a very good approximation, F_{ext} is found constant:

$$F_{ext}(a) = 2\pi R V(0) \quad (8)$$

Since the adhesion energy $w = -V(0) > 0$ the pull out force for the DMT theory [15] is then

$$F_{pullout} = -2\pi R w \quad (9)$$

In the DMT theory the work of adhesion results from the vertical motion (penetration) of the sphere in the interaction field, irrespective of the contact problem and especially of the contact radius.

1.2. Surface energy transfer – JKR

In the JKR model adhesion is a completely different mechanism involving *adhesion energy* coupled to the *contact area* and the release of elastic energy stored in the deformed punch. The JKR model can be viewed as a pull-back motion applied to the sphere inducing a peel action, as shown on Fig. 2. This pull-back motion at fixed contact radius is a flat punch displacement δ_{fp} . It results in the formation of a neck at the edge of the contact (Fig. 2). This neck is experimentally observed on soft solids in adhesion.

The adhesion energy is controlled by the neck height δ_{fp} as

$$2\pi a w = E^* \delta_{fp}^2 \quad (10)$$

where

$$E^* = \frac{E}{1 - \nu^2} \quad (11)$$

This equation is at the root of the JKR model [16]. This is a local approach to adhesion and the neck height depends upon the elastic response and adhesion energy but is completely independent upon the punch shape.

Linear superposition of the adhesionless contact for an arbitrary punch shape and the flat punch solutions provides the contact equations

$$\delta_{JKR}(a) = \delta_H(a) + \delta_{fp} \quad (12)$$

$$F_{JKR}(a) = F_H(a) + F_{fp}(a) \quad (13)$$

In contrast to the previous models the flat punch term offsets both Hertzian force *and* penetration. The correction to the Hertzian force, the flat punch force

term, is given by

$$F_{fp}(a) = \delta_{fp} S(a) \quad (14)$$

where the stiffness ² is

$$S(a) = 2aE^* \quad (16)$$

The pull out force for the JKR theory for a sphere of radius R is the minimum registered for Eq. 13 or

$$F_{pullout} = -\frac{3}{2}\pi R w \quad (17)$$

1.3. Domains of validity

Considering here a sphere of radius R , an order of magnitude estimate of the contact radius is obtained by equating Hertzian and adhesive force contributions in Eq. 4 or 13. Then

$$F_H(a) = \frac{4E^* a^3}{3R} \simeq \pi w R \quad (18)$$

As a result the typical contact radius is

$$a_c = \left(\frac{\pi w R^2}{E^*} \right)^{\frac{1}{3}} \quad (19)$$

and the typical penetration is

$$\delta \simeq \frac{a^2}{R} = \left(\frac{\pi^2 w^2 R}{E^{*2}} \right)^{\frac{1}{3}} \quad (20)$$

The gap shape Eq. 7 will deviate from the parabolic profile only for heights of the order of the penetration so that Eq. 8 applies when the interaction range

$$\delta_{int} \gg \left(\frac{\pi^2 w^2 R}{E^{*2}} \right)^{1/3} \quad (21)$$

For the JKR model, combining Eqs. 10 and 19 we observe that the JKR flat punch displacement is

$$|\delta_{fp}| \simeq \left(\frac{\pi w^2 R}{E^{*2}} \right)^{1/3} \quad (22)$$

²Regarding this stiffness note also that Eq. 10 is a special case of the compliance equation

$$2\pi a w = \frac{1}{2} \delta_{fp}^2 \frac{dS}{da} \quad (15)$$

which results from the differentiation of the elastic energy at fixed grip.

Now if the neck height δ_{fp} is large enough, which is typically the case for soft materials, then it spans the full interaction range, of order δ_{int} . A contact radius variation da results in a transfer of work $w d(\pi a^2)$ from the contact zone, in complete analogy with a peel test for example. The crack is in a steady state and the surface energy approach is vindicated.

Tabor [17] suggested to introduce a parameter comparing the flat punch displacement to the interaction range potential $\delta_{int} \simeq w/\sigma$. Denoting this parameter λ , we have

$$\lambda \equiv \frac{\delta_{fp}}{\delta_{int}} \simeq \frac{\sigma}{\left(\frac{wE^*2}{\pi R}\right)^{1/3}} \quad (23)$$

This parameter measures the impact of the interaction stresses on the surface deformations. The JKR case is obtained for large λ while small λ values characterize the DMT regime. In contrast to DMT, the JKR theory applies when interaction stresses are large and the materials compliant.

2. Cohesive Zone Models

In the general case, the relation between macroscopic variables is

$$\delta(a) = \delta_H(a) + \delta_{fp} \quad (24)$$

$$F(a) = F_H(a) + F_{fp}(a) + F_{ext}(a) \quad (25)$$

where Eq. 5 is valid. However if the flat punch displacement δ_{fp} is not zero, then the gap h is increased from the flat punch displacement and the contribution to Eq. 5 is reduced. Simultaneously in Eq. 10 only a fraction of the total adhesion energy is involved because steady state is not reached. Of course for a quantitative description to be obtained the details of the interactions between surfaces must be specified and at this point the cohesive zone model enters in the picture.

2.1. The double Hertz model

Here we consider a specific cohesive zone model, the double Hertz model. In the double Hertz model, the stress distribution in the cohesive zone is ellipsoidal.

With the present notation:

$$\sigma(r) = \begin{cases} -\sigma_0 \sqrt{\frac{c^2-r^2}{c^2-a^2}} & \text{if } a \leq r \leq c \\ 0 & \text{if } c < r \end{cases} \quad (26)$$

with $\sigma_0 > 0$. Greenwood and Johnson calculated the full solution by scaling Hertzian distributions by some ad hoc factor k . The factor k basically plays the role of the cohesive stress σ_0 but the form

$$\frac{k}{R} = \frac{\pi\sigma_0}{2E^*\sqrt{c^2-a^2}} \quad (27)$$

mixes parameters relevant to the punch and parameters relevant to the cohesive zone, which obscures the meaning of the various terms, especially in the self-consistency equation (Eq. 30). Below we briefly show how the double Hertz model can be derived from the cohesive zone stress distribution using auxiliary functions but before that, we summarize the main results of the double Hertz model [10], translated into the present notation:

1. penetration

$$\delta = \delta_H(a) - \frac{\pi\sigma_0}{2E^*} \sqrt{c^2-a^2} \quad (28)$$

2. force

$$F(a) = F_H(a) - \frac{2\pi\sigma_0}{3} \frac{c^3-a^3}{\sqrt{c^2-a^2}}. \quad (29)$$

3. self-consistency equation

$$w = \frac{1}{3} \left(\frac{1}{R} + \frac{\pi\sigma_0}{2E^*\sqrt{c^2-a^2}} \right) \frac{\sigma_0}{\sqrt{c^2-a^2}} I_H(c, a). \quad (30)$$

with

$$I_H(c, a) = (c-a)^2(c+2a) \quad (31)$$

We will now introduce the model with a rather general method in which adhesive elastic contacts are handled using auxiliary functions. We first show how the method applies to the double Hertz model then discuss some general features of adhesive contacts on the specific example of this cohesive zone model.

For an axisymmetric, elastic frictionless contact, we define two auxiliary functions [8, 11]

$$g(s) = \int_s^{+\infty} \frac{r\sigma(r)}{(r^2 - s^2)^{1/2}} dr, \quad (32)$$

$$\theta(s) = \frac{d}{ds} \int_0^s \frac{ru(r)}{\sqrt{s^2 - r^2}} dr, \quad (33)$$

Then mechanical equilibrium results in the relation

$$g(s) = \frac{E^*}{2} \theta(s) \text{ for all } s. \quad (34)$$

Note that in contrast to the equilibrium relation written in direct space, this relation is purely local.

2.1.1. Normal Surface Stresses

From Eq. 32 and the stress distribution Eq. 26, we calculate g *outside the contact zone*. The inverse form

$$\sigma(r) = -\frac{2}{\pi} \int_r^c \frac{g'(s)}{\sqrt{s^2 - r^2}} ds \quad (35)$$

directly suggests that for $a \leq r \leq c$

$$g'(r) = \frac{\pi}{2} \frac{\sigma_0}{\sqrt{c^2 - a^2}} r \quad (36)$$

so that $g(r)$ is parabolic:

$$g(r) = \begin{cases} \frac{\pi}{4} \sigma_0 \frac{r^2 - c^2}{\sqrt{c^2 - a^2}} & \text{if } a \leq r \leq c \\ 0 & \text{if } c < r \end{cases} \quad (37)$$

This simple analytical form for g is the very reason why the double Hertz model is so amenable.

2.1.2. Surface Displacements

For a given punch shape θ is known *inside the contact zone*. Indeed we find from Eq. 33 that

$$\theta(r) = \delta - \delta_H(r) \quad (38)$$

where the function $\delta_H(a)$ is the penetration for the adhesionless contact³ for a contact radius a . In particular it appears that $\theta(a)$ is the flat punch displacement of Eq. 10.

2.2. Contact Equations

Using Eq. 34, *continuity of the stress distribution at a* implies

$$g(a) = \frac{E^*}{2}\theta(a) \quad (39)$$

which determines the flat punch displacement. From Eq. 37 we obtain in the double Hertz model

$$g(a) = -\frac{\pi}{4}\sigma_0\sqrt{c^2 - a^2} \quad (40)$$

From what has been said so far, it is clear that the value of the auxiliary function g taken at $r = a$ is the key variable in the present approach. We will now investigate the meaning of $g(a)$ in more detail.

2.2.1. Penetration

From Eq. 39 we obtain the flat punch displacement as a function of $g(a)$

$$\delta_{fp} = \frac{2}{E^*}g(a) \quad (41)$$

which is negative, in agreement with the pull-back motion involved. Then Eq. 28 results.

2.2.2. Force

The two first terms in Eq. 25 are

$$F_H(a) + F_{fp}(a) = F_H(a) + 4ag(a) = F_H(a) - \pi\sigma_0a\sqrt{c^2 - a^2} \quad (42)$$

where the second term is the JKR-like flat punch force term (Eq. 13). The third term (the DMT-like external force term – Eq. 5) is given by

$$F_{ext}(a) = -\frac{\pi\sigma_0}{3\sqrt{c^2 - a^2}}(c - a)^2(2c + a). \quad (43)$$

Altogether all three contributions result in Eq. 29.

³As shown by inserting $g(a) = 0$ in Eq. 39

3. Self-Consistent Approach

Generally speaking, solving the elastic problem taking into account equation 6 exactly is tedious, and unnecessary [9]. Instead we resort to a weaker form of the same equation, imposing as additional condition that the spatial distribution should mimic the stress distribution derived from a reasonable interaction potential (Eq. 6). Based on the stress distribution given by Eq. 26 and enforcing the definition of adhesion energy [9], we obtain the following self-consistency equation

$$w = - \int_0^{+\infty} dz \sigma(z) = - \int_a^{+\infty} \sigma(r) \frac{dh(r)}{dr} dr \quad (44)$$

The calculation of the gap $h(r)$ is more involved. It is carried out by inverting Eq. 33 and the results are summarized in the appendix. The various contributions add up to Eq. 30.

As discussed previously [18], the first term results from the work of the interaction stresses in the Hertzian displacement field (linear in σ_0) while the second term is the work of the interaction stresses in the displacement field they have induced themselves (quadratic in σ_0). The first term is of DMT character while the second term is JKR (or fracture-like) in nature. Indeed the derivation of the relation between stress intensity factor and energy release rate is exactly the calculation of the work of the fracture stresses in the fracture displacement for a virtual crack motion [19].

In the large σ_0 limit $\epsilon \equiv c - a \ll a$ and the first DMT like term in the self consistency equation Eq. 30 is negligible. Then using Eqs. 40 and 41 the JKR equation Eq. 10 is recovered. Conversely in the small σ_0 limit

$$\frac{\sigma_0 c^2}{3R} \simeq w \quad (45)$$

and Eq. 25 reduces to Eq. 8. The gradual transition from purely external force contribution (DMT) to purely peeling effect (JKR) is illustrated on Fig. 3.

3.1. Surface stresses

The distribution of normal surface stresses (Fig. 4) for $r \leq a$ can be calculated through Eq. 35 resulting in

$$\sigma_z(r) = \frac{2}{\pi} \left\{ \left(\frac{E^*}{R} + \frac{\pi}{2} \frac{\sigma_0}{\sqrt{c^2 - a^2}} \right) \sqrt{a^2 - r^2} - \frac{\pi}{2} \frac{\sigma_0}{\sqrt{c^2 - a^2}} \sqrt{c^2 - r^2} \right\} \quad (46)$$

When $\epsilon = (c - a) \rightarrow 0$ the difference of the last two terms converges as

$$\sqrt{c^2 - r^2} - \sqrt{a^2 - r^2} \rightarrow \frac{a(c - a)}{\sqrt{a^2 - r^2}} \quad (47)$$

so that this contribution to the stress distribution converges as

$$\sigma_{zz}(r) \rightarrow \frac{2}{\pi} \frac{g(a)}{\sqrt{a^2 - r^2}} \quad (48)$$

where Eq. 40 with $\sqrt{c + a} \rightarrow \sqrt{2a}$ has been used. This is the flat punch stress distribution expected in the JKR limit, as demonstrated on Fig. 4.

Close to the crack tip, this stress distribution takes on the fracture-like distribution

$$\sigma_z \simeq \frac{K}{\sqrt{2\pi(a - r)}} \quad (49)$$

where the stress intensity factor

$$K = \frac{2g(a)}{\sqrt{\pi a}} \quad (50)$$

This result further illustrates the alternative role of $g(a)$ as an expression of the stress intensity factor.

3.2. The Carpick-Schwartz model

We also note in passing that all models describing the JKR-DMT transition are not cohesive zone models. From the previous considerations, we can conclude that the present theoretical framework is perfectly amenable to an attractive interaction resulting from the superposition of a very short range interaction in the JKR manner (adhesion energy w_1) and a very long range interaction in the DMT manner (adhesion energy w_2). The total adhesion energy is $w = w_1 + w_2$. The flat punch displacement will be determined by

$$2\pi a w_1 = E^* \delta_{fp}^2 \quad (51)$$

and the external force by

$$F_{ext}(a) = -2\pi R w_2 \quad (52)$$

from which the contact equations are derived as before. This result amounts to the Carpick-Schwarz [20, 21] model (CS), which were initially derived from an ad hoc form of the self consistency equation.

However, in the CS model, the stress distribution is the JKR stress distribution for the adhesion energy w_1 . In particular we point to the fact that this effective adhesive contact model spans the transition without addition of a physically motivated lengthscale as needed for more advanced contact models. The Tabor-like parameter defined as w_1/w_2 mimicks a DMT-JKR transition as shown by Carpick [20] and Schwarz [21], but only for the macroscopic contact variables. Indeed the singular stress distribution characteristic of the JKR model is maintained in the CS model. This is different from our previous attempt to include different lengthscales simultaneously [22]. Although the CS model provides helpful contact equations, at the macroscopic scale, it does not offer a useful solution for more complex issues such as dissipation at the crack tip, where the strain rate is mitigated by the finite size of the cohesive zone.

4. Conclusion

We have shown how the double Hertz model can be derived using the auxiliary function g and θ . The theory is used to illustrate the structure of adhesive contact theories. Adhesion is mediated both by the direct interaction through the gap and by the release of stored elastic energy as in fracture. The range of the cohesive stresses and the resulting size of the cohesive zone are the key lengthscales which determine the respective contributions of these two processes. This lengthscale impacts advanced models where material response is involved. In particular it is central to the modeling of velocity dependent adhesive contact of viscoelastic materials.

- [1] D. Maugis. Adhesion of spheres: The JKR-DMT transition using a dugdale model. *J. Colloid Interface Sci*, 150:243–69, 1992.

- [2] K. L. Johnson and J. A. Greenwood. An adhesion map for the contact of elastic spheres. *J. Colloid Interface Sci.*, 192:326–333, 1997.
- [3] C.Y. Hui, NJ Glassmaker, T. Tang, and A. Jagota. Design of biomimetic fibrillar interfaces: 2. Mechanics of enhanced adhesion. *Journal of The Royal Society Interface*, 1(1):35, 2004.
- [4] H. Gao, X. Wang, H. Yao, S. Gorb, and E. Arzt. Mechanics of hierarchical adhesion structures of geckos. *Mech. Mater.*, 37:275 – 285, 2005.
- [5] R. A. Schapery. A theory of crack initiation and growth in viscoelastic media. *International Journal of Fracture*, 11(1):141 – 159, 1975.
- [6] J. A. Greenwood and K. L. Johnson. The mechanics of adhesion of viscoelastic solids. *Phil. Mag.*, 43:697–711, 1981.
- [7] C. Y. Hui, J. M. Baney, and E. J. Kramer. Contact mechanics and adhesion of viscoelastic spheres. *Langmuir*, 14:6570–78, 1998.
- [8] E. Barthel and G. Haiat. A simple model for the adhesive contact of viscoelastic spheres. *Langmuir*, 18:9362–9370, 2002.
- [9] E. Barthel. On the description of the adhesive contact of spheres with arbitrary interaction potentials. *J. Colloid Interface Sci.*, 200:7–18, 1998.
- [10] J. A. Greenwood and K. L. Johnson. An alternative to the maugis model of adhesion between elastic spheres. *J. Phys. D - Appl. Phys.*, 31:3279–3290, 1998.
- [11] G. Haiat, M. C. Phan Huy, and E. Barthel. The adhesive contact of viscoelastic spheres. *J. Mech. Phys. Sol.*, 51:69–99, 2003.
- [12] A. S. Huguet and E. Barthel. Surface forces and the adhesive contact of axisymmetric bodies. *J. Adhesion*, 74:143–175, 2000.
- [13] M. D. Pashley. Further consideration of the dmt model for elastic contact. *Colloids Surf.*, 12:69–77, 1984.

- [14] Z. Zheng and J. Yu. Using the dugdale approximation to match a specific interaction in the adhesive contact of elastic objects. *J. Colloid Interface Sci.*, 310:27–34, 2007.
- [15] B. V. Derjaguin, V. M. Muller, and Yu. P. Toporov. Effect of contact deformation on the adhesion. *J. Colloid Interface Sci.*, 53:314, 1975.
- [16] K. L. Johnson, K. Kendall, and A. D. Roberts. Surface energy and the contact of elastic solids. *Proc. Roy. Soc. London A*, 324:301–313, 1971.
- [17] D. Tabor. Surface forces and surface interactions. *J. Colloids Interface Sci.*, 58:2, 1977.
- [18] E. Barthel. Elastic adhesive contact – JKR and more. *J. Phys. D: Appl. Phys.*, 41:163001, 2008.
- [19] B. Lawn and T. Wilshaw. *Fracture of Brittle Solids*. CUP, 1975.
- [20] R. W. Carpick, D. F. Ogletree, and Salmeron M. A general equation for fitting contact area and friction vs load measurements. *J. Colloid Interface Sci.*, 211:395–400, 1999.
- [21] U. D. Schwarz. A generalized analytical model for the elastic deformation of an adhesive contact between a sphere and a flat surface. *J. Colloid Interface Sci.*, 261:99–106, 2003.
- [22] E. Barthel. The adhesive contact of spheres: when the interaction is complex. *Colloids Surf. A*, 149:99–105, 1999.

Appendix: the gap and the self-consistency equation

The Hertzian gap is

$$h_H(r, a) = \frac{2}{\pi} \frac{1}{R} f_H(r, a), \quad (53)$$

where

$$f_H(r, a) \equiv \int_a^r ds \frac{(s^2 - a^2)}{\sqrt{r^2 - s^2}} = \left\{ \frac{a}{2} \sqrt{r^2 - a^2} + \left(\frac{r^2}{2} - a^2 \right) \arccos \left(\frac{a}{r} \right) \right\} \quad (54)$$

For the double Hertz model the gap is

$$\begin{aligned} h(r) &= \left(\frac{2}{\pi R} + \frac{\sigma_0}{E^* \sqrt{c^2 - a^2}} \right) f_H(r, a) \\ &\quad - \frac{\sigma_0}{E^* \sqrt{c^2 - a^2}} Y(r - c) f_H(r, c). \end{aligned} \quad (55)$$

For the self-consistency equation 44 the first term only in Eq. 55 contributes to the integral. We have to calculate

$$I = \int_a^c dr \sqrt{c^2 - r^2} \frac{\partial}{\partial f_H} r(r, a). \quad (56)$$

It can be shown that

$$I = \frac{\pi}{6} I_H(c, a), \quad (57)$$

where I_H is given by Eq. 31 Thus

$$w = \left(\frac{2}{\pi R} + \frac{\sigma_0}{E^* \sqrt{c^2 - a^2}} \right) \frac{\sigma_0}{\sqrt{c^2 - a^2}} I \quad (58)$$

and Eq. 30 results.

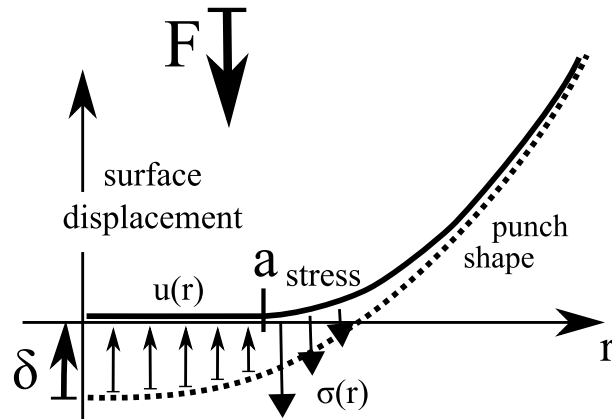


Figure 1: Schematics of an adhesive contact and the relevant boundary conditions: the macroscopic contact variables are the force F , the penetration δ and the contact radius a . The known normal surface displacement $u(r)$ inside the contact zone and the tensile normal surface stress $\sigma(r)$ outside the contact zone are schematized by two different types of arrows.

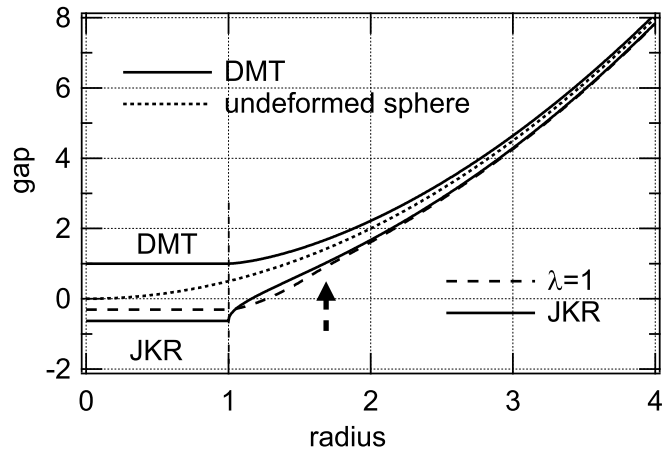


Figure 2: The gaps for the DMT and JKR limits, along with a solution of the double Hertz model with Tabor parameter $\lambda = 1$. Normalized forms were used with contact radius $a = 1$ and a sphere radius $R = 1$. A penetration offset has been applied so that all curves converge to the undeformed sphere (short dashes) at large radius. The arrow points to the edge of the cohesive zone in the double Hertz model.

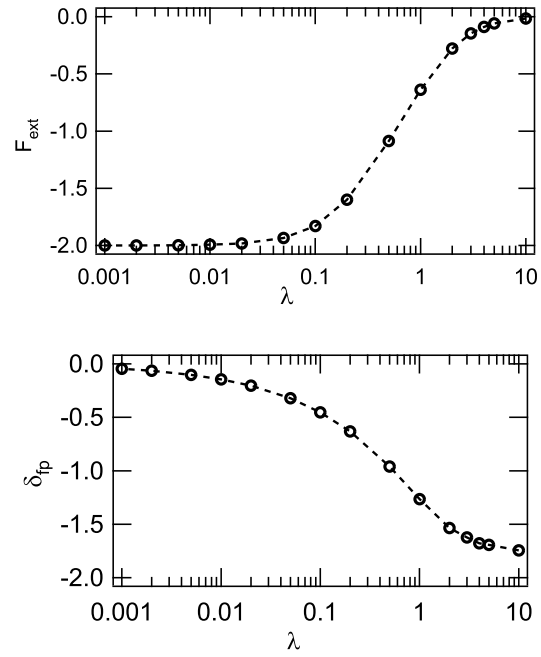


Figure 3: Evolution of normalized external force and flat punch displacement as a function of Tabor parameter λ . These two quantities exhibit inverse evolutions, which exemplifies the transition between the two regimes. For low values of the Tabor parameter, adhesion is dominated by the work of the external stresses into the rigid body displacement of the punch (DMT). For larger values, in contrast, interfacial energy is transferred at the crack tip through the stress singularity (JKR).

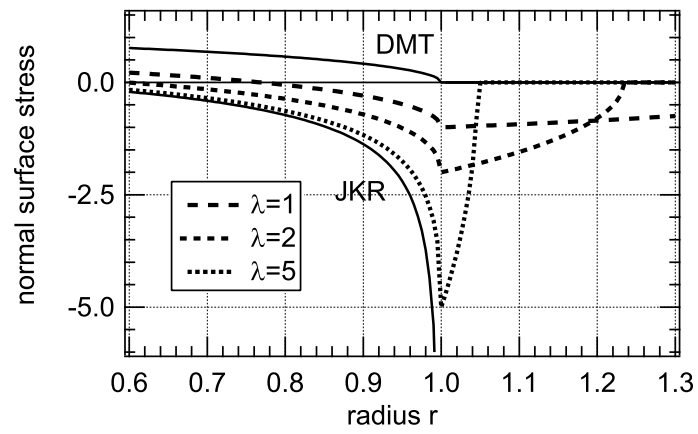


Figure 4: Stress distribution around the cohesive zone as a function of λ . The contact radius $a = 1$. The finite size of the cohesive zone, which physically speaking results from the decay length of the adhesion interactions, regularizes the JKR singularity.